

Supersolid phases in underdamped Josephson arrays: Quantum Monte Carlo simulations

Eric Roddick and David Stroud

Department of Physics, The Ohio State University, Columbus, Ohio 43210

(Received 28 October 1994; revised manuscript received 21 December 1994)

We carry out a quantum Monte Carlo study of Josephson arrays at temperature $T=0$ in the presence of an offset voltage between array and substrate. With diagonal and nearest-neighbor charge coupling, we find two types of insulating lobes with different types of charge order, and two types of superconducting regions. One is a supersolid with coexisting long-range phase coherence and checkerboard charge order. The supersolid phase is robust at half-filling. With next-nearest-neighbor coupling, there are two types of supersolid phase, one with checkerboard and one with striped charge order. Our phase diagram agrees with mean-field theory and with quantum Monte Carlo results of van Otterlo *et al.* in comparable regions of parameter space, but differs in detail from that of a Bose-Hubbard model with nearest-neighbor charging energies.

The “supersolid phase” (Refs. 1–6) is a possible state of Bose system in which two types of long-range order, denoted “diagonal” and “off-diagonal,” coexist. Typically, the diagonal order is a charge-density wave or other type of long-range charge order, while the off-diagonal order corresponds to a superconducting or superfluid phase. Such a phase can be realized, in principle, by an underdamped Josephson array in the presence of an offset voltage. In this case, the “diagonal” phase is a charge ordered state with a checkerboard pattern of Cooper pairs, while the “off-diagonal” state is a phase-coherent superconducting state. This system corresponds to a collection of interacting “soft-core” bosons, in the sense that multiple Cooper pairs are allowed to occupy a given grain. Another system thought to be describable in terms of a soft-core Bose Hamiltonian is ^4He adsorbed on the walls of a porous medium.⁷ In this case, the phase-coherent superfluid phase corresponds to off-diagonal order, while diagonal order is related to the local density of bosons, i.e., of ^4He atoms.

Recently, several groups have debated the existence of a supersolid phase in specific model Hamiltonians. For example, we have previously analyzed a soft-core Bose Hamiltonian, using a mean-field approximation,⁴ and at temperature $T=0$ found a supersolid phase over a broad range of parameters. The predicted range includes the so-called half-filled case (half-integer number of bosons per grain). van Otterlo and Wagenblast⁵ have studied the same model using a quantum Monte Carlo (QMC) method. They found a narrower supersolid region, which still includes the half-integer case. Batrouni *et al.* have studied a slightly different model at various Bose filling factors, and found a supersolid phase only at non-half-integer filling.

In this paper we show that these discrepancies are more apparent than real. We first show that the two models are actually inequivalent, having different commutation relations. Then, using QMC techniques, we show that the supersolid phase at half-filling is not just barely stable, but is, in fact, quite robust. We also show that our model permits multiple occupancy of bosons on a given site, which may help explain the different phase diagrams of the different models. Finally, we study other types of charge order, such as a

“striped” structure, which appears in our simulations when next-nearest-neighbor interactions are included.

We consider the model Hamiltonian^{4,5}

$$H = \frac{1}{2} \sum_{ij} U_{ij} (n_i - \bar{n})(n_j - \bar{n}) + \sum_{\langle ij \rangle} t [1 - \cos(\phi_i - \phi_j)], \quad (1)$$

where the first summation runs over all grains i and j . The first term represents the Coulomb interaction between charges on grains i and j , while the second denotes the Josephson coupling energy between nearest-neighbor grains. The constant \bar{n} is proportional to the offset voltage of the array with respect to a common ground potential and serves as a chemical potential for Cooper pair injection. The pair number n_i on grain i and the phase of the superconducting order parameter ϕ_i are canonically conjugate with commutation relations $[n_i, \phi_j] = -i \delta_{ij}$.

The Bose-Hubbard Hamiltonian is similar to Eq. (1):

$$H = \frac{1}{2} \sum_{ij} U_{ij} n_i n_j - \mu \sum_i n_i - \frac{1}{2} \sum_{\langle ij \rangle} (b_i^\dagger b_j + b_i b_j^\dagger), \quad (2)$$

where b_i^\dagger creates a soft-core boson at site i . In this model, the number operator $n_i = b_i^\dagger b_i$, where b_i and b_i^\dagger satisfy the usual Bose commutation relations: $[b_i, b_j^\dagger] = \delta_{ij}$. Another similar Hamiltonian is the spin-1/2 XXZ Heisenberg model,

$$H = \frac{1}{2} \sum_{ij} U_{ij} S_i^z S_j^z - h \sum_i S_i^z - \frac{1}{2} \sum_{\langle ij \rangle} (S_i^x S_j^x + S_i^y S_j^y), \quad (3)$$

where \mathbf{S} satisfies the usual commutation relations for spin operators and h is an externally applied magnetic field. Despite a superficial similarity, however, both these models actually are quite distinct from Eq. (1). Specifically, the X and Y components of i th “spin” in our model are represented by $\cos \phi_i$ and $\sin \phi_i$ and thus commute, whereas in both the Bose-Hubbard and spin-1/2 XXZ models these spin components do not commute. Furthermore, in the spin-1/2 XXZ system, the z component of the spin may take only two values, which limits the number of charges on each grain to either 0 or 1. (Hence this model is said to describe “hard-

core bosons.³⁾ The Bose-Hubbard Hamiltonian also restricts the number of particles on each grain, allowing only positive values. By contrast, in Eq. (1) the charge number can have any (positive or negative) integer value.

These distinctions may be particularly relevant at half-integer filling. At this filling, neither the Bose-Hubbard nor the spin-1/2 XXZ model can have a supersolid phase: once a checkerboard charge structure has formed, superfluid cannot flow without creating charges of 2 or -1 on some of the sites. By contrast, the model of Eq. (1) permits multiple occupancy, so that a supercurrent is allowed even in the presence of charge structure.

We have studied (1) at $T=0$ using the QMC technique of Ref. 8 to extend the calculations of Ref. 5 to a broader parameter regime. The partition function corresponding to (1) is written $Z = \text{Tr} e^{-\beta H}$, where $\beta = 1/k_B T$. The exponential is then broken up into a product of N_τ terms,

$$e^{-\beta H} = e^{-\beta H/N_\tau} e^{-\beta H/N_\tau} \dots e^{-\beta H/N_\tau}, \quad (4)$$

and an identity matrix is inserted between each exponential factor. To avoid a complex action, arising from the term linear in n_i , the identity matrix is written in a basis diagonal in the n_i 's. The off-diagonal terms (i.e., those originating from the Josephson coupling) are treated in the Villain approximation⁹ in which terms of the form $\exp(-\epsilon t \cos \Delta \phi)$ are replaced by $\sum_{m=-\infty}^{\infty} e^{im \Delta \phi} \exp(-m^2/2\epsilon t)$. The partition function then becomes $Z = \text{Tr} \exp(-S)$, where

$$S = \frac{\epsilon}{2} \sum_{ij,\tau} U_{ij} (n_{i,\tau} - \bar{n})(n_{j,\tau} - \bar{n}) + \frac{1}{2t\epsilon} \sum_{i,\tau} |\mathbf{J}_{i,\tau}|^2 \quad (5)$$

and $\epsilon = \beta/N_\tau$. The variables $(J_{i,\tau}^x, J_{i,\tau}^y, n_{i,\tau})$ can be treated as an integer-valued current field, because of the constraint imposed by the continuity equation $\Delta_\perp \cdot \mathbf{J} + \Delta_\tau n = 0$, where Δ_\perp and Δ_τ denote discrete gradients in the two spatial and one temporal directions. This procedure transforms an originally d -dimensional quantum problem into a $(d+1)$ -dimensional classical action (here $d=2$).

Typically, we study an $N \times N \times N_\tau$ lattice with $N = N_\tau = 6, 8, \text{ or } 10$, and periodic boundary conditions in all three directions. Our initial configuration has an average of \bar{n} charges per site. We use $\approx 10^5$ passes through the entire lattice for equilibration and evaluate averages using an additional 3×10^5 passes. The sample is equilibrated by slowly annealing from a temperature of $k_B T = 1.7U_0$ to $k_B T = 0.05U_0$, where the equilibrium averages are taken.

If only the diagonal and nearest-neighbor charging energies (denoted $2U_0$ and U_1) are nonvanishing, mean-field theory (MFT) for model (1) (Ref. 4) gives rise to four different types of order: a superconducting phase with no charge order at large values of the Josephson coupling; two Mott-insulating phases at small values of t , one with charge order (centered around half-integer \bar{n}) and one with no charge order; and finally, a supersolid phase in which the superconducting phase order coexists with charge order, also centered around half-integer \bar{n} . As U_1/U_0 increases, the two lobes centered at $\bar{n} = 1/2$ grow. The main features of the phase diagram have been verified using Monte Carlo simulations.⁵ However, the stability region for the supersolid phase is reduced in the simulation, relative to the mean-field

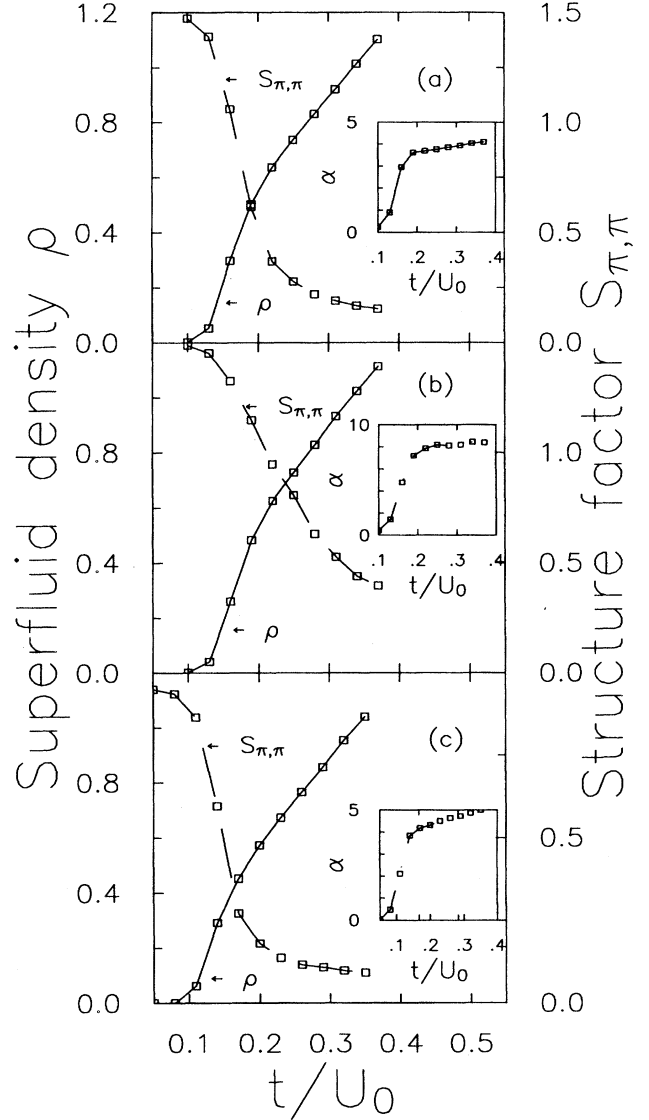


FIG. 1. Structure factor $S_{\pi,\pi}$ and superfluid density ρ as a function of t/U_0 for (a) $U_1/U_0=0.4$, $\bar{n}=1/2$; (b) $U_1/U_0 = 0.45$, $\bar{n}=1/2$; and (c) $U_1/U_0=0.4$, $\bar{n}=0.4$; nearest-neighbor coupling only. Also shown in the insets are the multiple occupancy order parameter $\alpha = \langle \sum_i n_i^2 - n_i \rangle$.

calculation. In order to confirm that this phase is indeed robust over a broad range of parameters, we have used the QMC method at several additional values of these parameters.

In Fig. 1(a), we plot the superfluid density $\langle |\sum_{i,\tau} J_{i,\tau}^x|^2 / (N^2 N_\tau) \rangle$ and the structure factor $S_{\pi,\pi} \equiv \langle \sum_{i,j} (n_i - \bar{n})(n_j - \bar{n})(-1)^{i-j} / (N^4 N_\tau) \rangle$ at $\bar{n} = 1/2$ as a function of the Josephson coupling t for $U_0 = 1$ and $U_1 = 0.4$. These plots indicate that there is a supersolid phase at half-filling, as predicted by MFT, but that, in agreement with Ref. 5, its width is smaller than MFT. To show the influence of multiple occupancy, we have also included as an inset to this plot an order parameter α which “measures” the possibility of occupancy other than 0 or 1:

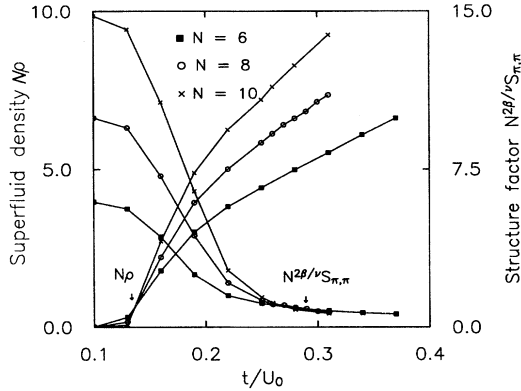


FIG. 2. Scaling plots of $N\rho$ and $N^{2\beta/\nu}S_{\pi,\pi}$ versus t/U_0 at $U_1/U_0=0.4$, $\bar{n}=0.5$, and $N=6, 8$, and 10 , assuming $\beta=0.21$, and $\nu=0.54$. Estimated critical points for onset of superconductivity and charge order are indicated by vertical arrows.

$\alpha = \langle \sum_i (n_i^2 - n_i) \rangle$. α is strictly zero if n_i is 0 or 1, but is greater than zero otherwise. We find that this order parameter remains zero in the nonsuperconducting region. In the superconducting region α becomes finite. By contrast, $\alpha \equiv 0$ for the spin-1/2 XXZ model and $\alpha \approx 0$ in the charge-ordered state at $\bar{n}=1/2$ of the Bose-Hubbard model.

Figure 1(b) shows the results for $U_1/U_0 = 0.45$ but still at half-integer filling. The “supersolid” region, where both the checkerboard charge order and superconducting phase coherence coexist, is much wider than in Fig. 1(a). Indeed, we have found that this region becomes even wider as U_1/U_0 approaches the limiting value of 0.5. Above 0.5, the Hamiltonian (1) is unbounded below (for a square lattice). By contrast, in both the XXZ and the Bose-Hubbard model, there appears to be no supersolid region at half-filling for any value of the parameters. We attribute the difference simply to the fact that these models have different commutation relations from our model.

In Fig. 1(c), we show a similar plot but at $U_1/U_0=0.4$, and $\bar{n}=0.4$, i.e., away from half-filling. In this case, the supersolid region is shifted to smaller t/U_0 , and may also be narrower than at half-filling. This possible narrowing differs from the results of van Otterlo and Wagenblast’s results, but is consistent with our mean-field results.

To pinpoint the phase transitions in Fig. 1(a), we have done finite-size scaling for $N \times N \times N_\tau$ lattices with $N=6, 8$, and 10 , and $N_\tau=N^z$ and the critical exponent $z=1$, as expected at half-filling.⁵ To accomplish the scaling, we use the relations⁸ $\rho = N^{-1}\bar{\rho}(\delta N^{1/\nu}, N_\tau/N)$, where $\bar{\rho}$ is a universal scaling function, ν is the critical exponent for the coherence length, and $\delta \equiv (t - t_c)/t_c$ is the distance to the transition; and $S_{\pi,\pi} = N^{-2\beta/\nu}\bar{S}(\delta N^{1/\nu}, N_\tau/N)$, where β is the order-parameter exponent. Superconductivity sets in at the common crossing point of all the plots of $N\rho$ for different lattice sizes. Similarly, the critical point for the onset of charge order is the point where the plots of $N^{2\beta/\nu}S_{\pi,\pi}$ all cross. Such plots are shown in Fig. 2 for $N=N_\tau=6, 8$, and 10 , using the expected values⁵ $\beta=0.21$ and $\nu=0.54$. There is a clear critical point for superconductivity near $t/U_0=0.13$, and a nearly equally clear one for charge order near 0.28.

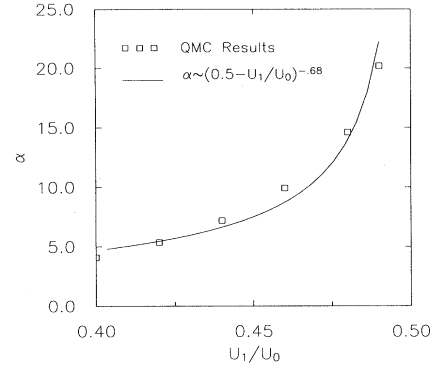


FIG. 3. Plot of $\alpha = \langle \sum_i n_i^2 - n_i \rangle$ as a function of U_1/U_0 for $t/U_0=0.35$ and $\bar{n}=0.5$.

Thus a broad supersolid region of coexisting charge and superfluid order exists at $\bar{n}=0.5$ for this range of parameters.

It is of interest to follow the behavior of α as the parameters \bar{n} and U_1/U_0 are varied. For fixed \bar{n} , as U_1/U_0 increases from 0.4 to 0.45, α doubles in value. This behavior can be clearly seen in Fig. 3. Evidently the larger the supersolid region, the larger α becomes. In addition, for fixed U_1/U_0 , α increases as \bar{n} varies from 0.5 (half-filling) to 0.4. This behavior arises because the energy cost for having -1 Cooper pairs on any given grain is smaller for $\bar{n}=0.4$ than for $\bar{n}=0.5$. Likewise, as U_1/U_0 increase, the energy cost of having a number of Cooper pairs other than 0 or 1 decreases, allowing α to increase.

Finally, we have also considered the case of nonzero *next-nearest-neighbor* coupling U_2 (cf. Fig. 4). In this case, there are two different types of possible charge order, denoted “checkerboard” and “striped” order. Checkerboard order is signaled by a nonzero Fourier component $S_{\pi,\pi}$ while striped order corresponds to nonzero $S_{0,\pi}$ or $S_{\pi,0}$. Such order has also been considered by Batrouni *et al.*⁶ for the Bose-Hubbard model. In Fig. 4 we have plotted both Fourier components versus U_2/U_0 at $\bar{n}=0.5$, $U_1/U_0=0.45$, and $t/U_0=0.19$. Clearly either type of order can coexist with superconductivity in a supersolid phase at $\bar{n}=1/2$, but not simultaneously. There is a change from checkerboard to striped order near $U_2/U_0=0.15$. Over the entire region, the

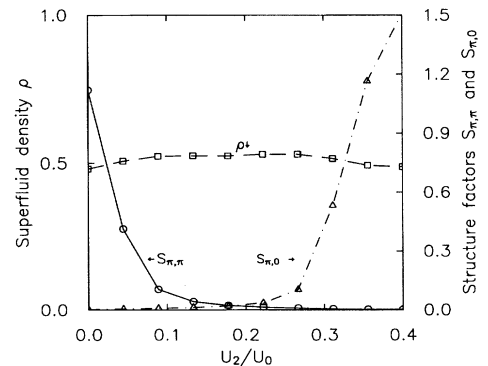


FIG. 4. Structure factors $S_{\pi,\pi}$ and $S_{0,\pi}$, and superfluid density ρ as a function of U_2/U_0 for $U_1/U_0 = 0.45$, $t/U_0 = 0.19$, and $\bar{n}=0.5$.

superfluid density remains nearly independent of U_2/U_0 . The two types of supersolid are separated by a narrow region which is strictly superfluid, and not either type of supersolid.

To summarize, using QMC simulations, we have confirmed our earlier mean-field results that a simple model of soft-core bosons has a supersolid phase in a narrow region of the phase diagram, at half-integer boson filling, and in a comparable region at other than half-filling. Our results, obtained using a slightly different Monte Carlo algorithm, agree with those of Ref. 5 in corresponding regions of the phase diagram. We have also shown that the supersolid phase at half-filling is very robust: as the variable U_1/U_0 increases, the supersolid region covers an ever broader part of the phase diagram. Finally, we have studied the effects of next-nearest-neighbor charge interactions. As this coupling constant increases, a striped charge order sets in. We find that a supersolid phase can be produced with striped order, analogous to the checkerboard ordered supersolid arising from nearest-

neighbor coupling. Our results differ somewhat from a recent study of a Bose-Hubbard model,⁶ because of differences in commutation relations and the possibility of multiple charge occupancy.

Although our model is intended to describe underdamped Josephson arrays, our results might be relevant to many systems having two competing types of order in noncommuting variables. Thus they may conceivably be relevant to systems in which superconductivity competes with antiferromagnetism, or more exotic types of order.

We acknowledge useful conversations with Dr. S. Ryu. This work has been supported by the National Science Foundation, through Grants No. DMR90-20994 and No. DMR94-02131, and by the Midwest Superconductivity Consortium at Purdue University through D.O.E. Grant No. DE-FG90-02-ER-45427. Calculations were carried out, in part, on the CRAY Y-MP of the Ohio Supercomputer Center.

¹M. Matsuda and T. Tsuneto, Prog. Theor. Phys. Suppl. **46**, 411 (1970).

²Kao-Shien Liu and M. E. Fisher, J. Low Temp. Phys. **10**, 655 (1973).

³C. Bruder, R. Fazio, and G. Schön, Phys. Rev. B **47**, 342 (1993).

⁴E. Roddick and D. Stroud, Phys. Rev. B **48**, 16 600 (1993).

⁵A. van Otterlo and K. Wagenblast, Phys. Rev. Lett. **72**, 3598

(1994).

⁶G. Batrouni, R. Scalettar, G. Zimanyi, and A. Kampf (unpublished).

⁷M. P. A. Fisher, P. B. Weichman, G. Grinstein, and D. S. Fisher, Phys. Rev. B **40**, 546 (1989).

⁸E. Sorensen *et al.*, Phys. Rev. Lett. **69**, 828 (1992).

⁹J. Villain, J. Phys. (Paris) **36**, 581 (1975).